A -78dBm Sensitivity Super-regenerative Receiver at 96 GHz with Quench-controlled Metamaterial Oscillator in 65nm CMOS

Yang Shang[1], Haipeng Fu[2], Hao Yu[1]*, and Junyan Ren[2]

[1]School of Electrical and Electronic Engineering, Nanyang Technological University, Singapore, 639798

[2]State Key Laboratory of ASIC and System and School of Microelectronics, Fudan University, Shanghai, China 200433

haoyu@ntu.edu.sg; jyren@fudan.edu.cn

***Abstract* — One high-sensitivity CMOS super-regenerative receiver is demonstrated for 96GHz mm-wave imaging based on high-Q metamaterial oscillator. Compared to traditional LC-tank based oscillator, the metamaterial oscillator is developed by folded-differential transmission-line loaded complimentary split-ring resonator (FDTL-CSRR). With formed sharp stop-band, standing-wave is established with high EM-energy storage at mm-wave region for high-Q oscillatory amplification. As such, one high-sensitivity 96 GHz super-regenerative receiver is realized in 65nm CMOS with measurement results of: -78 dBm sensitivity, 0.67 fW/Hz$^{0.5}$ NEP, 8.5 dB NF, 2.8mW power consumption and 0.014 mm^2 core area.**

***Index Terms* — metamaterial oscillator, high Q and high sensitivity, super-regenerative receiver, mm-wave imaging.**

I. Introduction

Recent researches [1]-[4] have demonstrated great potential of both active and passive millimeter-wave (mm-wave) imaging system to detect covered substances for either bio-medical or security detections. Compared to the other semiconductor technologies like GaAs, the standard CMOS technology is considered as the most cost-effective solution for large detector-arrayed mm-wave imaging system with on-chip image processing. However, due to loss in propagation path (80-90 dB) under limited transmitting power, the CMOS mm-wave imaging system requires sufficient receiver sensitivity.

The receiver sensitivity is determined by the minimum input signal power as described by Rayleigh-Hean thermal noise model: $S = KTB \cdot NF$. Here, S is the sensitivity, K is the Boltzmann constant, T is the ambient temperature (K), B is the bandwidth and NF is the noise figure. As such, a sharper bandwidth B under a given noise figure NF can result in a high sensitivity (or smaller S) receiver. Due to low frame-rate of mm-wave imaging video, the narrow or sharp bandwidth B is desired for high sensitivity of receiver. As such, the super-regenerative receiver is a promising candidate for mm-wave imaging applications [1][2] since high-sensitivity can be obtained by a quench-controlled oscillator to achieve an oscillatory amplification with sharper bandwidth than direct conversion receivers[3][4]. As illustrated in Fig.1, the quench-controlled oscillator consists of one resonator block and one frequency-selected positive feedback network. When periodical quench signal is applied, the averaged output signal power is amplified with the RF input signal power.

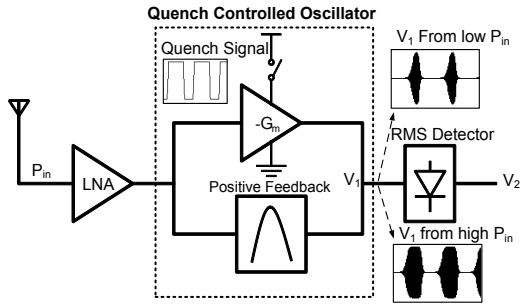

Fig.1. Super-regenerative receiver block diagram and operation principle.

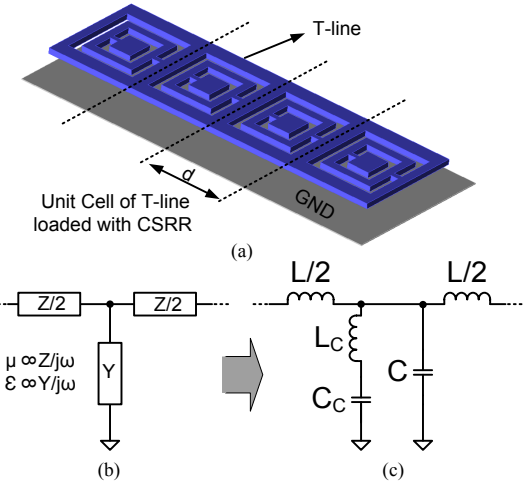

Fig. 2. (a) On-chip implementation of T-line loaded with CSRR, (b) T-line model, (c) Unit-cell equivalent circuit of T-line loaded with CSRR

Note that the bandwidth B of one super-regenerative receiver is mainly determined by the quality factor (Q) of

the resonator by: $Q = f_0/B$, where f_0 is the resonance frequency. As such, on-chip high-Q resonator is desired for the high-sensitivity super-regenerative receiver design. As shown in this paper, one metamaterial resonator is developed based on a novel structure of folded-differential transmission-line loaded with complementary split-ring resonator (FDTL-CSRR), which is further deployed in the super-regenerative receiver for high-sensitivity. It is demonstrated with the measured -78dBm sensitivity at 96GHz in UMC 65nm CMOS.

II. High-Q FDTL-CSRR Oscillator

Metamaterial was first demonstrated in 2001 [5] with split-ring resonator (SRR), which shows negative permeability (μ) at resonance frequency, and is deployed for on-chip application in [6]. According to the complementary theory, complementary split-ring resonator (CSRR) was also proposed in 2004 [7] with negative permittivity (ε) at resonance frequency. The CSRR structure can be considered as an electric dipole excited by the electric field (E-Field) along the ring axis. CSRR with negative ε can be deployed as the load for a host with positive μ such as a transmission-line (T-line). As such, the electric plasma can be formed when ε is negative and μ is positive with a sharp stop-band at the vicinity of resonance. As such, the wave propagating at the host T-line is perfectly reflected at the CSSR load with an established standing-wave. Therefore, the EM-energy can be stored with low-loss transferring between the host and load, which results a high-Q resonator.

A. T-line loaded with CSRR

Note that for the on-chip implementation of T-line loaded with CSRR (TL-CSRR), CSRRs are engraved on the signal trace of T-line on the top most metal layer as shown in Fig. 2a. The metamaterial property for TL-CSRR can be analyzed by T-line model [8].

T-line is modeled by cascading unit-cells with distributed series impedance (Z) and shunt admittance (Y), which determine permittivity (ε) and permeability (μ) as depicted in Fig. 2b. The equivalent circuit of TL-CSRR is depicted in Fig. 2c. L and C are the intrinsic series inductance and shunt capacitance of T-line, while L_C and C_C are the equivalent inductance and capacitance of CSRR resonator. By comparing Fig. 2b and Fig. 2c, one can observe that μ is always positive as $\mu \infty L/d$, where d is the length of TL-CSRR unit-cell; and ε is negative when $\varepsilon \infty (\frac{C_C}{\omega^2 L_C C_C} + C)/d$<0, of which the frequency range is

$$\sqrt{\frac{1}{(C + C_C)L_C}} < \omega < \sqrt{\frac{1}{C_C L_C}}. \quad (1)$$

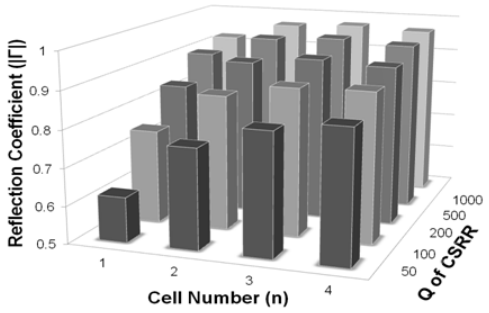

Fig. 3. Reflection coefficient of T-line loaded with CSRR unit-cells

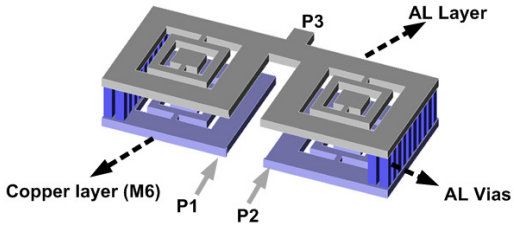

Fig. 4. Layout for on-chip implementation of FDTL-CSRR

As such, electric plasma is formed in this frequency range. The EM-energy propagating into the TL-CSRR will be reflected with established standing wave. The reflection coefficient (|Γ|) depends on the number of cascading TL-CSRR unit-cells and also the Q value of loaded CSRR. Based on circuit level simulation, Fig.3 shows the study of TL-CSRR at 100 GHz resonance frequency with following observations. First, the reflection coefficient |Γ|can be improved by high-Q loaded CSRRs. Second, for a given Q value of loaded CSRR, the overall reflection coefficient can be improved by cascading more unit-cells.

B. Folded Differential T-line loaded with CSRR

The TL-CSRR structure cannot be directly used for a super-regenerative receiver design due to the following reasons. First, the single-ended approach is not preferred because of large common-mode noise; second, additional area overhead is required when cascading more unit-cells.

To address these two issues, a folded-differential T-line loaded with CSRR (FDTL-CSRR) structure is proposed in this paper. As shown in Fig. 4, two cascaded CSRR unit-cells are folded into the top most metal layers (AL and M6) and are connected by AL vias in between. The ADS momentum EM-simulator is used to verify the S-parameters of the proposed FDTL-CSRR structure in Fig. 4. The metamaterial properties are extracted from the EM simulation results according to the procedure in [9]. Note that only the real parts of extracted ε and μ are considered in the analysis as the imaginary parts are introduced by the loss of T-line. As shown in Fig. 5, the electric plasma is formed with negative ε and positive μ at the vicinity of 104 GHz resonance. It forms a band with deep rejection of

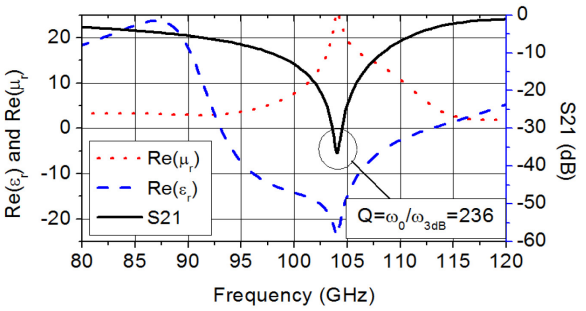

Fig. 5. Characterization of FDTL-CSRR by EM-simulation

-36 dB and narrow bandwidth of 0.44 GHz. The Q factor can be calculated as 236 by: $Q = \omega_0/\omega_{3dB}$.

III. High Sensivitiy Super-regenerative Receiver

The high-Q FDTL-CSRR metamaterial resonator results in sharp bandwidth that can improve sensitivity of the super-regenerative receiver. One super-regenerative receiver with DTL-CSRR is designed in UMC standard 65 nm CMOS process to demonstrate this sensitivity improvement. The schematic of the proposed receiver is illustrated in Fig. 7. Firstly, FDTL-CSRR with the unit-cell size of 60 μm × 60 μm is connected to cross-coupled M2 and M3 NMOS transistors to form a differential oscillator. The tail current of the oscillator is quench-controlled by M4 NMOS transistor. In order to provide a sufficient driving current and head-room for the oscillation, the size of M4 NMOS transistor is designed 4 times larger than M2 or M3 NMOS transistor. Note that the minimum channel length of 60nm is applied for all transistors.

The remaining circuit consists of one input low-noise-amplifier (LNA) and also one envelop detector. The M1 NMOS transistor serves as a common-source LNA and also provides reverse isolation between the RF input and the oscillator. The input of M1 NMOS transistor is matched to 50 Ω by T-line-based matching network. Note that the size of M1 NMOS transistor is much smaller than that of M2 or M3 NMOS transistors to avoid unbalanced oscillation. Moreover, M5 and M6 are the only PMOS transistors used in this circuit to serve as a differential envelop detector. Their sizes need to be small to reduce the capacitive loading of the oscillator. In order to isolate 1/f noise and reduce the capacitance loading from M5 and M6, the differential oscillation signal is capacitively coupled to the envelop detector by MOM capacitors C1 and C2. This also enables the gates of M5 and M6 to be biased externally, which brings the flexibility of output reference tuning and also detection optimization. In addition, there are two λ/4 stubs at 96 GHz connected to the output, which can improve the isolation of the oscillation signal.

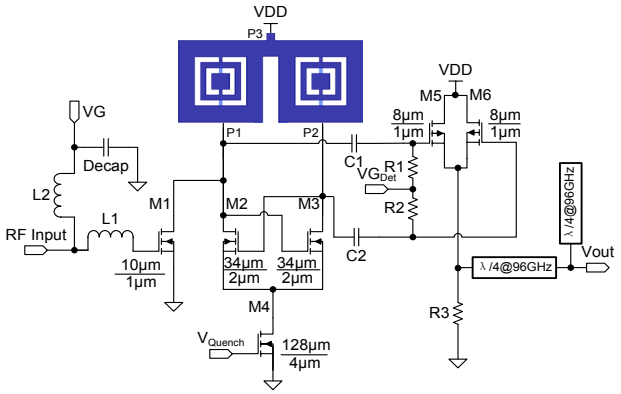

Fig. 6. Schematic of super-regenerative receiver with FDTL-CSRR oscillator

IV. Measurements and Discussion

As shown in Fig. 6, the super-regenerative receiver with FDTL-CSRR was fabricated in UMC 1P6M bulk 65 nm CMOS process. The core chip area is 0.014 mm^2; and the total area is 500 μm × 440 μm including all testing PADs. The receiver is measured on CASCADE Microtech Elite-300 probe station. The RF signal is provided by Agilent PNA-X (N5247A) with T/R module (N5260). A 12.5MHz sinusoid quench-control signal is applied by function generator (AFG3022) with voltage swept in 0~250 mV. The receiver operates under 1V power supply and the power consumption is observed as 2.8 mW.

Good input power matching is also important for the NF reduction and sensitivity improvement. The measured S11 remains below -10 dB from 81 GHz to 104 GHz as shown in Fig. 9. As a result of utilizing the high-Q FDTL-CSRR, narrow bandwidth of 560 MHz is observed around the center frequency of 95.5 GHz. Moreover, an almost linear response is observed in the plot of normalized Vout versus input power (Pin) by Fig. 9.

In addition as shown in Fig.9, the sensitivity of receiver is found to be -78 dBm in the measurement. The noise equivalent power (NEP) is defined as signal power in one hertz bandwidth that gives unity signal-to-noise ratio, which is equivalent to $S/\sqrt{B}$ and is found to be 0.67 fW/Hz$^{0.5}$. Finally, the noise figure is found to be 8.5 dB by S/KTB at room temperature of 290 K.

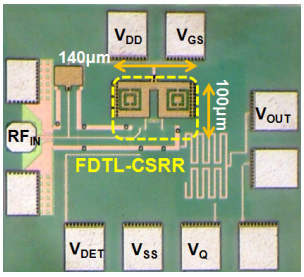

Fig. 7. Chip photo of 96GHz super-regenerative receiver

TABLE I
PERFORMANCE COMPARISON WITH RECENTLY PUBLISHED RECEIVERS ABOVE 90 GHZ

	[3]	[4]	[1]	[2]	**This work**
Technology	65nm CMOS	65nm BiCMOS	65nm CMOS	65nm CMOS	65nm CMOS
Frequency (GHz)	94	94	144	183	95.5
Sensitivity (dBm)	-66	-57	-74	-72.5	**-78**
Noise Figure(dB)	N/A	12	10.2	9.9	8.5
Bandwidth (GHz)	23	26	0.94	1.4	0.56
NEP (fW/Hz$^{0.5}$)	N/A	10.4	1.3	1.51	0.67
Power (mW)	93	200	2.5	13.5	**2.8**
Core Area (mm^2)	0.31	1.25	0.021	0.013	0.014

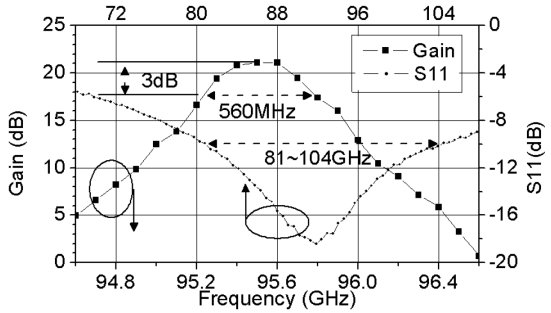

Fig. 8. Measurement results of super-receiver: i) output voltage when a -20 dBm tone is swept through bandwidth; ii) and also input S11parameters

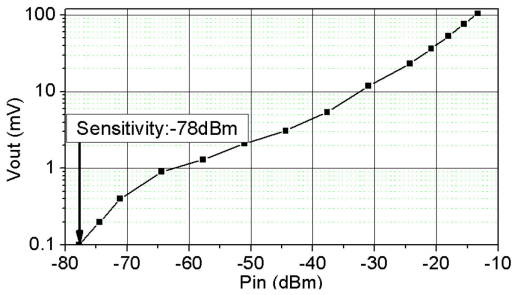

Fig. 9. Vout of super-receiver when a 95.5 GHz tone is swept from sensitivity level to -13 dBm

As shown in TABLE I, the measurement results of the proposed receiver are compared to the recently published mm-wave imaging receivers above 94 GHz [1-4]. The proposed receiver has achieved the best sensitivity, noise figure and NEP with almost the smallest power consumption and also the core chip area. Specifically, compared to the results from LC-tank resonator based super-regenerative receiver in [1], our high-Q metamaterial oscillator by FDL-CSRR has achieved more than 40% sharper bandwidth with 4dB higher sensitivity.

V. CONCLUSION

One high-sensitivity 96GHz super-regenerative receiver is demonstrated in 65nm CMOS with the use of metamaterial based high-Q resonator (FDTL-CSRR). Compared to the traditional LC-tank resonator, the high-Q and compact FDTL-CSRR results in narrower bandwidth and improved sensitivity for the super-regenerative receiver, which is implemented in UMC 65nm CMOS with 0.014 mm^2 of the core chip area. Measurement results show that the receiver has achieved: -78 dBm sensitivity, 0.67 fW/Hz$^{0.5}$ NEP, 8.5 dB NF and 2.8 mW power consumption. The compact size with improved sensitivity is ideal for the application of large-arrayed mm-wave imaging in CMOS.

ACKNOWLEDGEMENT

The authors acknowledge the support from MediaTek for the UMC 65nm CMOS tape-out, and fund by MOE Tier-1 RG 26/10 grant from Singapore. The authors appreciate the measurement support by Wei-Meng Lim at VIRTUS IC Design Centre of Excellence.

REFERENCES

[1] A. Tang, Z. Xu, Q. J. Gu, Y.-C. Wu, and M. C. F. Chang, "A 144 GHz 2.5mW Multi-Stage Regenerative Receiver for mm-Wave Imaging in 65nm CMOS," in *IEEE RFIC*, 2011.

[2] A. Tang, M. C. F. Chang, "183GHz 13.5mW/Pixel CMOS Regenerative Receiver for mm-Wave Imaging Applications," in *IEEE ISSCC*, 2011.

[3] K.W. Tang, M. Khanpour, P. Garcia, C. Garnier and S.P. Voinigescu, "65-nm CMOS, W-Band Receivers for Imaging Applications," in *IEEE CICC*, 2007.

[4] L. Gilreath, V. Jain, H.-C. Yao, L. Zheng, and P. Heydari, "A 94-GHz Passive Imaging Receiver using a Balanced LNA with Embedded Dicke Switch," in *IEEE RFIC*, 2010.

[5] R. A. Shelby, D. R. Smith, and S. Schultz, "Experimental Verification of a Negative Index of Refraction," *Science,* vol. 292, no. 5514, p. 77–79, 2001.

[6] D. Cai, Y. Shang, H. Yu, J. Ren and K. S. Yeo, "A 76 GHz Oscillator by High-Q Differential Transmission Line Loaded with Split Ring Resonator in 65-nm CMOS," in *IEEE SIRF*, 2013.

[7] F. Falcone, T. Lopetegi, J. Baena, R. Marques, F. Martin, and M. Sorolla, "Effective negative- epsiv; stopband microstrip lines based on complementary split ring resonators," *IEEE Microwave and Wireless Components Letters, vol. 14, no. 6, pp.,* vol. 14, no. 6, p. 280 – 282, 2004.

[8] A. Lai, T. Itoh, and C. Caloz, "Composite right/left-handed transmission line metamaterials," *IEEE Microwave Magazine,* vol. 5, no. 3, pp. 34-50, Sep. 2004.

[9] D. R. Smith, D. C. Vier, T. Koschny, and C. M. Soukoulis, "Electromagnetic parameter retrieval from inhomogeneous metamaterials," *Physical Review E,* vol. 71, p. 036617, 2005.